EPR-ENDOR Characterization of (O-17, H-1, H-2) Water in Manganese Catalase and Its Relevance to the Oxygen-Evolving Complex of Photosystem II

7 AUTHORS, INCLUDING:

Vladimir Grigoryants
University at Albany, The State University of …
34 PUBLICATIONS 637 CITATIONS

SEE PROFILE

Charles P Scholes
University at Albany, The State University of …
81 PUBLICATIONS 2,020 CITATIONS

SEE PROFILE

William K. Myers
University of Oxford
28 PUBLICATIONS 264 CITATIONS

SEE PROFILE

James W Whittaker
Oregon Health and Science University
96 PUBLICATIONS 3,959 CITATIONS

SEE PROFILE

EPR-ENDOR Characterization of (^{17}O, ^{1}H, ^{2}H) Water in Manganese Catalase and Its Relevance to the Oxygen-Evolving Complex of Photosystem II

Iain L. McConnell[1], **Vladimir M. Grigoryants**[2], **Charles P. Scholes**[2,*], **William K. Myers**[2,†], **Ping-Yu Chen**[1,‡], **James W. Whittaker**[3], and **Gary W. Brudvig**[1,*]

[1]Department of Chemistry, Yale University, P.O. Box 208107, New Haven, Connecticut 06520-8107

[2]Department of Chemistry, University at Albany, State University of New York, 1400 Washington Avenue, Albany, New York 12222

[3]Department of Science and Engineering, School of Medicine, Oregon Health and Science University, 20000 N.W. Walker Road, Beaverton, Oregon 97006

Abstract

The synthesis of efficient water-oxidation catalysts demands insight into the only known, naturally occurring water-oxidation catalyst, the oxygen-evolving complex (OEC) of photosystem II (PSII). Understanding the water oxidation mechanism requires knowledge of where and when substrate water binds to the OEC. Mn catalase in its Mn(III)-Mn(IV) state is a protein model of the OEC's S_2 state. From ^{17}O-labeled water exchanged into the di-μ-oxo di-Mn(III,IV) coordination sphere of Mn catalase, CW Q-band ENDOR spectroscopy revealed two distinctly different ^{17}O signals incorporated in distinctly different time regimes. First, a signal appearing after two hours of ^{17}O exchange was detected with a 13.0 MHz hyperfine coupling. From similarity in the time scale of isotope incorporation and in the ^{17}O μ-oxo hyperfine coupling of the di-μ-oxo di-Mn(III,IV) bipyridine model (Usov, O. M.; Grigoryants, V. M.; Tagore, R.; Brudvig, G. W.; Scholes, C. P. *J. Am. Chem. Soc.* **2007**, *129*, 11886-11887), this signal was assigned to μ-oxo oxygen. EPR line broadening was obvious from this ^{17}O μ-oxo species. Earlier exchange proceeded on the minute or faster time scale into a non-μ-oxo position, from which ^{17}O ENDOR showed a smaller 3.8 MHz hyperfine coupling and possible quadrupole splittings, indicating a terminal water of Mn(III). Exchangeable proton/deuteron hyperfine couplings, consistent with terminal water ligation to Mn(III), also appeared. Q-band CW ENDOR from the S_2 state of the OEC was obtained following multi-hour ^{17}O exchange, which showed a ^{17}O hyperfine signal with a 11 MHz hyperfine coupling, tentatively assigned as μ-oxo-^{17}O by resemblance to the μ-oxo signals from Mn catalase and the di-μ-oxo di-Mn(III,IV) bipyridine model.

*To Whom Correspondence Should be Addressed: Gary Brudvig, gary.brudvig@yale.edu. Charles Scholes, cps14@albany.edu.
†Current Address: Department of Chemistry, University of California, 1 Shields Avenue, Davis, California 95616-0935
‡Current Address: Department of Chemistry, National Chung-Hsing University, 250 Kuo-Kuang Road, Taichung, Taiwan 402, ROC

Introduction

Efficient solar energy-driven water-oxidation catalysts represent a very promising solution to the problem of generating renewable solar fuels,[1, 2] cheaply and on a large scale.[3–5] A starting point for such catalytic systems is the photosystem II (PSII) oxygen-evolving complex (OEC).[6] Composed of four Mn ions and a calcium ion, in addition to a proteinaceous ligation environment, the OEC oxidizes in a multistep reaction two water molecules with the energy from four photons of visible light.

Catalytic hypotheses and concomitant model development have been greatly aided by crystallographic structural information on PSII at a resolution down to 1.9 Å.[7–9] However, radiation damage has interfered with identification of the substrate water-binding sites. Identification of these sites is key to understanding the mechanism by which waters are activated for O-O bond formation. EPR spectroscopy can provide information on the binding of water/hydroxo/oxo species to the metal ions in the OEC, and these data may correlate with the substrate waters by comparison to the substrate exchange rates measured by mass spectrometry.[10–14]

The paramagnetic S_2 state of the OEC has a characteristic 1.80 T wide, 18+ line CW X-band EPR difference spectrum (S_2 minus S_1) or 'multiline signal', centered at g = 2.[15] An early EPR study detected broadening of this signal due to exchange of ^{17}O from ^{17}O-labeled water into the OEC.[16] This initial work showed that oxygen from water could interact with the manganese ions in the OEC. More recent studies have provided evidence for ^{17}O that exchanged from ^{17}O-labeled water into the OEC. X-band ESEEM (Electron Spin Echo Envelope Modulation) provided evidence for ^{17}O in the OEC with a hyperfine coupling of ~ 5 MHz.[17] This ESEEM signal was assigned as a terminal water ligated by π bonding to Mn(III),[17] based on the relation of the ^{17}O hyperfine couplings to those found for terminal water π bonded to low spin ferric cytochrome P450.[18] X-band HYSCORE (Hyperfine Sublevel Correlation) spectroscopy measurements on the OEC exchanged with ^{17}O-water showed a single pair of structureless features assigned as a ^{17}O coupling of ≈ 10 MHz.[19] However, while our present submission was in revision, an Addition/Correction was published using a ^{15}N substitution to show that the 2008 Su *et al.*[19] nominal ^{17}O HYSCORE signal actually derived from a ^{14}N spectral subtraction artifact.[20]

Di-μ-oxo Mn(III)-Mn(IV) bipyridine had been investigated as a simple chemical model of the OEC which lacks the complexity of that higher nuclearity cluster because it has μ-oxo oxygens but no terminal waters. Mass spectrometry confirmed that the μ-oxo ligands of this Mn(III)-Mn(IV) bipyridine model complex exchanged from ^{18}O-labeled water.[21] CW Q-band ENDOR and X-band EPR line broadening experiments revealed a ^{17}O hyperfine coupling of 12.8 MHz.[22] Given the breadth of the ENDOR line shape, we would take this hyperfine coupling as an estimate of the isotropic coupling. Thus, to date, the most reliable ^{17}O μ-oxo hyperfine coupling has been reported for the di-μ-oxo Mn(III)-Mn(IV) bipyridine model, for which mass spectrometry experiments confirm that the μ-oxo oxygen can exchange with isotopically enriched oxygen from water.[21]

As evidenced by rapid mass spectroscopic detection of $^{18}O_2$ product, two substrate ^{18}O-waters were found to exchange very quickly into the OEC itself, with product formation times of ~0.01 s and 0.5 s for a fast and a slow site respectively (in the S_2 state).[10–14] It is not clear where these catalytically relevant, rapidly exchanging water binding sites of the

OEC are located. There is resonance Raman evidence for a slower oxygen isotope exchange occurring on the order of tens of minutes into a Raman-detectable μ-oxo group localized in the OEC.[23] The mass spectroscopic study on the di-μ-oxo Mn(III)-Mn(IV) bipyridine model which had been dissolved in acetonitrile showed that oxygen ligand exchange into the di-μ-oxo groups from microliter quantities of ^{18}O-water occurred in about 20 min.[21] In the same study[21] terminal water ligand exchange rates of the di-μ-oxo Mn(III)-Mn(IV) terpy model complex could not be resolved, but the μ-oxo ligand exchange time of 400 s from this terpy model compound was the shortest time measured for di-μ-oxo models.

The rate of water exchange into a di-μ-oxo di-Mn system could be affected by an aqueous environment, proteinacious ligation, seclusion from the bulk phase, and electrostatic effects on pKa, all factors not under control in the organic solvent of the model work of Tagore *et al.*[21, 24] An improved model, also having the potential for terminal water ligation, could have a similar di-μ-oxo di-Mn center imbedded inside a soluble protein, and Mn catalase (MnCat) was chosen for that model.

The location and environmental character of a di-Mn di-μ-oxo center is known in the proteinaceous system of MnCat; the positions of both bridging oxygens, protein ligands, terminal water, and potentially critical second sphere amino acids are crystallographically known, as shown in Figure 1. MnCat is a 29.6 kDa hexamer forming-protein found in *Lactobacillus plantarum*[25] and also *Thermus thermophilus.*[26] It contains a di-Mn catalytic core with solvent derived aquo, hydroxo[27] or μ-oxo bridges,[28] depending on the oxidation state of the Mn. Under catalytic conditions, the Mn core oscillates between (II,II) and (III,III) oxidation states to disproportionate peroxide in a ping-pong mechanism.[29, 30] The enzyme can be oxidized beyond the (III,III) state by treatment with hydrogen peroxide and hydroxylamine[25, 31] or KIO_4.[26, 32, 33] This form of the enzyme, while catalytically inactive, is EPR active,[32, 34–36] producing a 16-line signal at g = 2 which is diagnostic of antiferromagnetically coupled Mn(III)-Mn(IV).[26, 33] EXAFS of this form of MnCat has also indicated a decrease in the Mn-Mn distance consistent with oxidation of one manganese to Mn(IV),[37] and this decrease was consistent with the Mn(III)-Mn(IV) distance found in di-μ-oxo models.[38] Advanced paramagnetic resonance studies have already been performed on MnCat in the (III,IV) state,[37, 39,40] but the ^{17}O ENDOR signals from potential μ-oxo or terminal water sites of MnCat have not been reported.

With the goal of learning about the mechanism of water binding and O_2 production in PSII, this work is focused on using ENDOR and EPR spectroscopy to characterize the binding and exchange of ^{17}O from ^{17}O-enriched water into both terminal and μ-oxo sites of MnCat. Data for this proteinaceous structural mimic of PSII provides the background to understand water exchange into PSII, its time course, locale, and catalytic relevance.

Materials and Methods

Preparative Methods

MnCat Preparation—MnCat was isolated from *L. plantarum* according to published procedures.[25, 41] The superoxidized Mn(III)-Mn(IV) state of MnCat was prepared with minor modifications as previously described.[25, 27, 31] MnCat was oxidized by redox cycling in the presence of hydrogen peroxide and hydroxylamine. Briefly, MnCat (0.1 mM active sites in 50 mM potassium phosphate buffer pH 7, containing 0.1 mM EDTA) was dialyzed against 1 L of 0.1 mM hydroxylamine and 0.1 mM H_2O_2 at 4 °C for 4 h. The protein was then transferred to 1 L of fresh 0.1 mM H_2O_2 solution (two changes), and finally, dialyzed overnight against 50 mM potassium phosphate buffer, pH 7, containing 0.1 mM EDTA. The sample, concentrated to 90 mg mL^{-1} (3 mM active sites), was then combined with a known volume of $H_2{}^{16}O$ or $H_2{}^{17}O$ for CW X-band EPR experiments. For Q-band ENDOR, $H_2{}^{17}O$

and glycerol; $H_2^{16}O$ and glycerol; or D_2O and deuterated glycerol (99% deuterium enrichment, Cambridge Isotope Laboratories, MA) were added. (Glycerol at 50% vol/vol is a glassing agent that prevents aggregation of paramagnetic centers upon freezing.) After addition of reagents, the sample was frozen at 77 K. Exchange time with the added $H_2^{17}O$ reagent was monitored to differentiate between short exchange periods (1–5 min) and long-term exchange (> 2 hours). $H_2^{17}O$ was supplied at 90 % enrichment from Cambridge Isotope Laboratories. Exchange of D_2O was accomplished in about a minute and the sample frozen; the sample was then unfrozen, deuterated glycerol added, and refrozen in about 5 minutes.

Photosystem II Preparation—Dark-adapted PSII membranes were prepared by the method of Berthold *et al.*[42] The membranes were brought in 2.0 mm i.d., 2.4 mm o.d. quartz EPR-ENDOR tubes to a final concentration of 10–20 mg chl/mL and a ~74 % concentration of exchangeable $H_2^{17}O$ with a method outlined in Supporting Information, Figure 1S. Following dark adaptation for 24 hours, samples were frozen by plunging in liquid nitrogen. To achieve the S_2 state for both the $H_2^{17}O$ sample and the $H_2^{16}O$ control, samples were illuminated for 1 min in an acetone bath at 200 K with a xenon arc lamp.

X-band EPR Methods

Mn-Cat cw X band EPR—Samples were stored at 77 K. CW X-band EPR scans were acquired on a Bruker ELEXSYS E500 EPR spectrometer equipped with a SHQ resonator and an Oxford ESR-900 helium-flow cryostat. The 16-line EPR signal was recorded at 7.5 K with the following instrumental parameters: microwave frequency 9.38 GHz, modulation frequency 100 kHz, modulation amplitude 3 G, microwave power 5 mW.

Photosystem II CW X band EPR—Following creation of the S_2 state by photoillumination, the EPR line widths of S_2 state samples enriched in $H_2^{17}O$ were compared with those of with non-enriched $H_2^{16}O$ samples. EPR scans were acquired as for MnCat.

CW Q-band ENDOR Methods

Spectroscopic Methods—CW Q-band (34.1 GHz) ENDOR measurements were performed under dispersion (χ'), rapid passage, field-modulated conditions with a cryogenically tunable TE011 Q-band resonator[43] at 2 K as previously reported.[22, 44, 45] For study of PSII, S_2 samples were transferred from liquid N_2 on a specially designed wand into the He-filled ENDOR cavity in the dark within 3 min of illumination. In this method of CW ENDOR, one monitors the radio-frequency (RF)-induced change in the rapid-passage, 100 kHz field modulated dispersion EPR signal as the frequency of the RF field is swept. RF power is pulsed with 100 μsec on/900 μsec off, with a peak power that is generally 20 W. Through previous experience we have determined that strongly coupled protons (coupling 4 MHz), ^{14}N, and ^{17}O are best resolved with a higher field modulation 2.5 Gauss p.t.p. (peak-to-peak)[22, 44, 45] while weakly coupled nuclei, notably deuterons here, are best resolved with smaller field modulation 0.5 Gauss p.t.p.[44] The frequencies of ENDOR features were determined from the average frequency of spectra taken with increasing and with decreasing frequency sweeps. CW field-modulated ENDOR has higher sensitivity than pulse methods for broad ENDOR signals, such as those of ^{17}O.[46] However, pulse methods, not available to us, appear to give better resolution of small detailed couplings, such as those of deuterons.[47] We are aware that CW ENDOR, as carried out in pumped liquid helium, can also be subject to baseline artifacts from RF and field modulation-induced heating.

First-Order ENDOR Theory—A nucleus, N, with spin I, e.g., ^{17}O (I = 5/2) or ^{14}N (I = 1), can be described by a Spin Hamiltonian of the form:

$$\text{Hnucl} = {}^{N}A_{xx}I_xS_x + {}^{N}A_{yy}I_yS_y + {}^{N}A_{zz}I_zS_z + {}^{N}P_{xx}\,I_x{}^2 + {}^{N}P_{yy}\,I_y{}^2 + {}^{N}P_{zz}\,I_z{}^2 + {}^{N}g_n\beta_n\mathbf{H}\cdot\mathbf{I}. \quad (1)$$

Where β_n is the nuclear Bohr magneton and ${}^{N}g_n$ is the nuclear g-value (${}^{1}g_n = 5.585$, ${}^{2}g_n = 0.8574$, ${}^{14}g_n = 0.4038$, ${}^{17}g_n = -0.7572$, ${}^{1}\nu = 52.928$ MHz, ${}^{2}\nu = 8.124$ MHz, ${}^{14}\nu = 3.816$ MHz, ${}^{17}\nu = 7.178$ MHz at 1.2431 T) for protons, deuterium, ^{14}N, and ^{17}O, respectively. ${}^{N}A_{xx}$, ${}^{N}A_{yy}$, and ${}^{N}A_{zz}$ are the components of the hyperfine tensor, and for nuclei with $I > \frac{1}{2}$, ${}^{N}P_{xx}$, ${}^{N}P_{yy}$, and ${}^{N}P_{zz}$, are the components of the quadrupolar tensor, where ${}^{N}P_{xx} + {}^{N}P_{yy} + {}^{N}P_{zz} = 0$. [${}^{N}P_{zz} = (3e^2q_{zz}{}^{N}Q/h)/(4I(2I-1))$ where e is the electronic charge; h is Planck's constant; ${}^{N}Q$ is the nuclear quadrupole coupling constant of a particular nucleus; I is the nuclear spin operator, and q_{zz} is the electric field gradient (EFG) along the "z" direction, a direction which may coincide for ^{14}N or ^{17}O with a bonding direction.] This terminology for Spin Hamiltonian parameters follows that used in our recent publications.[44, 45, 48, 49]

^{17}O ENDOR Frequencies and Hyperfine Analysis

To first order, the ^{17}O ENDOR frequencies will be:

$$\begin{aligned}{}^{17}\nu^{+}{}_{\text{ENDOR}} &= |{}^{17}A/2 + {}^{17}\nu| \\ &|{}^{17}A/2 + {}^{17}\nu \pm 3\,{}^{17}P| \qquad (2a) \\ &|{}^{17}A/2 + {}^{17}\nu \pm 6\,{}^{17}P|\end{aligned}$$

$$\begin{aligned}{}^{17}\nu^{-}{}_{\text{ENDOR}} &= |{}^{17}A/2 - {}^{17}\nu|. \\ &|{}^{17}A/2 - {}^{17}\nu \pm 3\,{}^{17}P| \qquad (2b) \\ &|{}^{17}A/2 - {}^{17}\nu \pm 6\,{}^{17}P|\end{aligned}$$

The ${}^{17}\nu^{+}{}_{\text{ENDOR}}$ branch has been the branch generally observed by Q-band CW rapid passage ENDOR on biologically relevant complexes,[46, 50–52] including the μ-oxo oxygens of the Mn(III)-Mn(IV) bipyridine dimer.[22] For those μ-oxo oxygens of the Mn(III)-Mn(IV) bipyridine dimer, the ${}^{17}\nu^{-}{}_{\text{ENDOR}}$ branch is close to zero frequency because of the near cancellation of $|{}^{17}A/2| \approx 6.4$ MHz and ${}^{17}\nu = 7.18$ MHz at 1.243 T). Relevant details of ^{17}O quadrupole and anisotropic hyperfine couplings are provided in the discussion and the Supporting Information.

^{14}N ENDOR Frequencies and Hyperfine Analysis

The first-order expressions for spin 1 ^{14}N ENDOR frequencies are:

$$\begin{aligned}{}^{14}\nu^{+}{}_{\text{ENDOR}} = |{}^{14}A/2 \pm 3/2\,{}^{14}P + {}^{14}\nu| \qquad (3a)\end{aligned}$$

$$\begin{aligned}{}^{14}\nu^{-}{}_{\text{ENDOR}} = |{}^{14}A/2 \pm 3/2\,{}^{14}P - {}^{14}\nu| \qquad (3b)\end{aligned}$$

where ${}^{14}A$ is the hyperfine coupling, ${}^{14}P$ the quadrupolar coupling, and ${}^{14}\nu$ is the ^{14}N nuclear Zeeman frequency. For ^{14}N nitrogen, as opposed to protons, the hyperfine term, ${}^{14}A/2$, rather than the nuclear Zeeman term ${}^{14}\nu$, is the dominant term measured by ENDOR. As with ^{17}O, for CW rapid passage Q-band ENDOR, the ${}^{14}\nu^{+}{}_{\text{ENDOR}}$ branch is frequently the branch observed.

Protons/Deuteron Frequencies and Hyperfine Analysis

The frequencies of proton or deuteron ENDOR features, $^1\nu_{ENDOR}$ or $^2\nu_{ENDOR}$, center, to first order, at the respective free proton or free deuteron nuclear Zeeman frequency, $^1\nu$ or $^2\nu$, and in the proton or deuteron ENDOR spectra we show the spectra centered at $^1\nu$ or $^2\nu$. For example, taking ^1A as the proton hyperfine coupling, one finds that the frequencies, $^1\nu^\pm_{ENDOR}$, are split away from the nuclear Zeeman frequency by $\pm 1/2\,^1A$ for protons coupled to the electron spin ½ doublet. Proton ENDOR frequencies, occurring as "+" or as "−" Zeeman branches, are:[53]

$$^1\nu^\pm_{ENDOR} = |^1\nu \pm\, ^1A/2| \quad (4)$$

With the neglect of small quadrupolar terms, a similar expression holds for deuterons:

$$^2\nu^\pm_{ENDOR} = |^2\nu \pm\, ^2A/2| \quad (5)$$

First-order expressions hold here because $^1\nu > |^1A/2|$ and $^2\nu > |^2A/2|$.

The strong, largely dipolar coupling to terminal water protons localized on the Mn(III) of the (2-OH-3,5-Cl$_2$-SALPN)$_2$ Mn(III)-Mn(IV) complex has previously been resolved by ENDOR-ESEEM measurements.[40, 54] The theory to explain the terminal water dipolar coupling, called extended dipole theory, incorporates the quantum mechanical projection factors for spin localized on the Mn(III) (S = 2) and Mn(IV) (S = 3/2) where these two ions are an antiferromagnetically coupled S = ½ pair. (The projection factor expresses the spin on an individual metal ion in terms of the total spin of the dimer. See, for example, the discussion and formula A3 on p. 4923, Khangulov *et al.*[40]) The theory provides the diagonalized hyperfine tensor[54] where both metal ions contribute in a non-colinear fashion to the dipolar Hamiltonian. A more complete discussion of the extended dipole method applied to ^{17}O–μ-oxo and to the terminal water protons in MnCat is provided in the Supporting Information.

Results

X-band EPR ^{17}O Line Broadening of MnCat

The first derivative CW X-band spectra were examined in the ^{16}O- and ^{17}O-exchanged states. The extent of broadening from the ^{17}O ligand is clear in Figure 2, which compares the overlaid line shapes of the ^{16}O-exchanged and ^{17}O-exchanged. The broader line width implies ^{17}O exchanged into the Mn(III)-Mn(IV) coordination sphere.

CW Q-band ^{17}O ENDOR of MnCat

CW rapid-passage Q-band ENDOR was obtained for water-derived ligands that exchanged into the active site of MnCat. (Q-band rapid-passage EPR of the 16-line spectra of MnCat are shown in Figure 2S of the Supporting Information.) Figure 3A provides evidence for the appearance after a two hour exchange of ^{17}O-water of a broad signal labeled ^{17}O$_A$, similar in line shape and ENDOR frequency to the ^{17}O from the μ-oxo oxygens in the di-μ-oxo Mn(III)-Mn(IV) bipyridine model complex.[22] The frequency of ^{17}O$_A$ is 13.7 ± 0.5 MHz, and this ENDOR frequency translates via Eq. 2a into a ^{17}O hyperfine coupling of 13.0 ± 1.0 MHz. To give insight into the approximate time course and origin for appearance of peaks, the MnCat sample was exchanged with ^{17}O-water for ~ 1 min, and as shown in Figure 3B, the higher frequency ^{17}O$_A$ feature near 14 MHz was then not present but features in the 7–11 MHz region were. When ^{16}O-water was used, a peak in the 6–7 MHz region remained, as

shown in Figure 3C. This remaining peak had an ENDOR frequency of 6.5 ± 0.3 MHz, and its ^{14}N coupling per Eq. 3 for $^{14}\nu^+$ is $^{14}A = 5.4 \pm 0.6$ MHz. This coupling is consistent with the coupling of $^{14}A = 5.75$ MHz recently reported by multi-frequency ESEEM and assigned to the histidine nitrogen ligated to Mn(III) of *L. plantarum* MnCat.[39] Although there is evidence from Figure 3C for a broad underlying baseline in the 10–25 MHz region, neither of the peaks, $^{17}O_A$ and $^{17}O_B$, was at all evident in this baseline.

Figure 3S in the Supporting Information provides a comparison of spectra from the same sample as that of Figure 3A at two different magnetic fields, H = 1.243 T near the center of the EPR pattern and H = 1.267 T at its high field end. Other than a difference in intensity, the ENDOR spectra at the two fields in Figure 3S are essentially identical. A more highly resolved spectrum for this two-hour ^{17}O-exchanged sample is shown in the Supporting Information, Figure 4S, where there is still the $^{17}O_A$ peak near 14 MHz, but where there is evidence for lower frequency features in the 7–11 MHz region, notably those labeled $^{17}O_B$.

By use of lower field modulation in the CW ENDOR technique, higher resolution of the $^{17}O_B$ signal than that in Figure 3B is provided in the inset adjacent to Figure 3B using the sample prepared with 1 min ^{17}O exchange. The ^{17}O hyperfine coupling of the $^{17}O_B$ peak labeled with an arrow in the inset near 9 MHz was 3.8 ± 0.6 MHz. Above 10 MHz there were two shoulders noted in the inset to 3B with splittings of about 1.3 MHz, while overlap with the ^{14}N signal prevented additional resolution of any ^{17}O details below 9 MHz. In the Supporting Information, Figure 5S, a comparison is made of the spectrum of the inset to Figure 3B showing the $^{17}O_B$ signals and the MnCat sample prepared with $H_2^{16}O$ which shows the ^{14}N signal but not $^{17}O_B$ signals.

CW Q-band – Proton and Deuteron ENDOR of MnCat

A comparison of CW proton ENDOR from a sample prepared in protonated buffer to a sample prepared in deuterated buffer provided evidence for exchangeable protons at the active site. Detailed features, especially the starred outlying ones, were best resolved in the first derivative presentation of Figure 4. (The standard absorption-like ENDOR spectra before a derivative was numerically taken are shown as Figure 6S in the Supporting Information.) These outlying features, per Eq. 4, had hyperfine couplings of 17.2 ± 0.4 and 12.2 ± 0.4 MHz, larger than any previously reported from MnCat by frequency-modulated X-band ENDOR of the 1990's,[40] but comparable with the largest component of the anisotropic proton hyperfine tensor of terminal water ligated to Mn(III) in the (2-OH-3,5-Cl$_2$-SALPN)$_2$ Mn(III)-Mn(IV) dimer.[54] There may be broad underlying exchangeable features with proton hyperfine couplings (A_3) less than 10 MHz, but such features are obscured by non-exchangeable protons.

Evidence for exchangeable protons implied that there are corresponding exchangeable deuterons, and so ENDOR from exchangeable deuterons was sought near the deuteron Larmor frequency, $^2\nu = 8.12$ MHz, as shown in the inset to Figure 4. The CW deuteron ENDOR spectrum does not have the resolution or signal to noise of the proton spectrum, but it complements the proton ENDOR information and shows evidence of exchangeable deuterons. Protons with hyperfine couplings less than ~10 MHz are obscured in Figure 4 by non-exchangeable protons; whereas, the associated deuterons with couplings less than about 1.5 MHz (i.e., with a splitting away from $^2\nu$ of ~±0.75 MHz) are obvious even at low resolution and occur only from exchanged deuterons.

CW Q-band ^{17}O and ^{14}N ENDOR of the S$_2$ State of PSII

The ^{17}O information from MnCat provided motivation to obtain corresponding information from the S$_2$ state of PSII. Twenty four hours of exchange with $H_2^{17}O$ produced a definite,

light-induced ^{17}O hyperfine interaction from the S_2 state of PSII. A comparison (Figure 5) of S_2 ENDOR signals from PSII samples, respectively exchanged with $H_2{}^{16}O$ and $H_2{}^{17}O$, indicated a ^{17}O ENDOR signal at 12.8 ± 0.5 MHz, similar to that of MnCat here and to that of the previously reported ^{17}O-bridged Mn^{III}-Mn^{IV} bipyridine dimer.[22] The ^{17}O hyperfine coupling, derived via Eq. 2a, was $|^{17}\mathbf{A}| = 11 \pm 1$ MHz. An additional signal occurred at 7.3 ± 0.2 MHz from all S_2 samples, and its hyperfine coupling, assigned to ^{14}N and interpreted by Eq. 3, is $|^{14}\mathbf{A}| = 7.0 \pm 0.4$ MHz. This coupling is similar to the 7.2 MHz coupling reported from ESEEM studies of the OEC and assigned to the D1-H332 histidine nitrogen [55, 56] that is ligated to Mn No. 2 (Numbering system of Sproviero *et al.*[57])

Discussion

μ-oxo ^{17}O Hyperfine Interaction

There are now <u>three</u> structurally related systems into which ^{17}O has been exchanged from ^{17}O-water. The first is the di-μ-oxo Mn(III)-Mn(IV) bipyridine complex, known by mass spectroscopic quantitation to exchange both of its μ-oxo oxygens with isotopically enriched ^{18}O-water.[21, 24] It has no other oxygen ligands to exchange and, therefore, its ^{17}O ENDOR signal has to be μ-oxo. Both ENDOR and EPR line broadening of the ^{17}O-di-μ-oxo Mn(III)-Mn(IV) bipyridine complex showed a ^{17}O hyperfine coupling of 12.8 MHz.[22] For the di-μ-oxo Mn(III)-Mn(IV) bipyridine complex, the time for induction of the ^{17}O signal by exchange from ^{17}O-water was of order twenty minutes. The present study on MnCat showed an even longer time for induction of its ^{17}O signal ($^{17}O_A$ in Figure 3A), a signal having a very similar hyperfine coupling to that of the di-μ-oxo Mn(III)-Mn(IV) bipyridine complex of 13.0 MHz. MnCat is known to have a di-μ-oxo center,[27, 37] and based on the slow ^{17}O kinetic induction from ^{17}O-water and the similar ^{17}O hyperfine to that in the di-μ-oxo model, we assign the ^{17}O ENDOR signal ($^{17}O_A$ in Figure 3A) of MnCat to a μ-oxo oxygen in its Mn(III)-Mn(IV) center.

The S_2 state of the OEC has resonance Raman evidence for slow oxygen isotope exchange into a μ-oxo group,[23] and the implication is that there is at least one μ-oxo oxygen in the OEC that can exchange very slowly with solvent. The OEC showed a similar ^{17}O signal to the slowly exchanging ^{17}O signal of the ^{17}O-μ-oxo Mn(III)-Mn(IV) bipyridine and also to the $^{17}O_A$ signal in MnCat. The hyperfine coupling from the ^{17}O signal in the OEC was 11 MHz, which is ~ 15 % less than the hyperfine coupling of the ^{17}O-μ-oxo in the di-μ-oxo Mn(III)-Mn(IV) bipyridyl complex. A simple explanation for the smaller coupling in the OEC could be that the spin in the tetranuclear Mn center of the OEC is delocalized beyond one di-μ-oxo bridged Mn(III)-Mn(IV) pair.[58, 59] The tetranuclear center of the OEC is less well defined at present than the bi-nuclear center of Mn(III)-Mn(IV) bipyridine, and so we can not be as confident in our assignment of our ^{17}O ENDOR signal from the OEC. However, it is extremely tempting to suggest that the ^{17}O ENDOR signal of the OEC may be from a μ-oxo oxygen within the OEC, in particular, to the μ-oxo oxygen between the distal Mn(III) (Mn No. 4) and its adjacent Mn(IV) partner (Mn No. 2),[9, 57] which is the oxygen postulated to originate from a "slow exchangeable water" (See Fig. 13 of Kulik *et al.*[58]).

Beyond the obvious presence of high-valent Mn in all of these systems, their common aspect is μ-oxo oxygen. μ-oxo oxygen mediates via covalent superexchange the antiferromagnetic coupling between paramagnetic metals,[60] and the detailed electronic nature of antiferromagnetic superexchange is critical to redox/catalytic properties.[61] Broken symmetry DFT has been used to predict spin density at μ-oxo oxygens and pathways for superexchange. Hyperfine couplings for ^{55}Mn, ^{14}N, and ^{1}H, have been calculated, but not for ^{17}O.[62–65] Given the central importance of μ-oxo oxygens to all these high-valent multi-

manganese complexes, especially the OEC, prediction of the μ-oxo ^{17}O hyperfine coupling would be a sensitive test of the capabilities of broken symmetry DFT.

The antiferromagnetically coupled Fe(III)-Fe(IV) center of ribonucleotide reductase (RNR) has been the subject of considerable previous ^{17}O ENDOR.[46, 66] The μ-oxo ^{17}O hyperfine tensor in RNR was found to be highly anisotropic ($^{17}A_{xx}$, $^{17}A_{yy}$, $^{17}A_{zz} = 0$, 23.5, 23.5 MHz). The μ-oxo ^{17}O isotropic hyperfine coupling of RNR is 15–16 MHz,[44] comparable to the isotropic coupling we estimate from our μ-oxo ^{17}O findings. There was additional hyperfine coupling to a terminal ^{17}O-water of the Fe(III) with an isotropic component about double that of the μ-oxo, and the μ-oxo ^{17}O of RNR was distinguished kinetically from the terminal ^{17}O-water through rapid freeze quench methods to follow rapid incorporation from $^{17}O_2$. The RNR system has advantages over the multi-Mn system that lead to better ENDOR signal to noise and resolution. Due to absence large ^{55}Mn nuclear hyperfine couplings, the RNR EPR signal at Q-band is only ~0.1 T wide[67] versus 1.2–1.8 T wide for di-Mn(III)-Mn(IV), accounting for greater EPR-ENDOR sensitivity for RNR. The RNR system has sufficient g-anisotropy for good angle selection of ^{17}O ENDOR hyperfine anisotropy; this is not the case for di-Mn(III)-Mn(IV). The μ-oxo couplings of RNR should be larger than those in di-Mn(III)-Mn(IV) systems because Fe tends to be more covalent than Mn and because the S = 5/2 ferric ion has a spin-containing d$(x^2\text{-}y^2)$ orbital directed for σ bonding toward the oxygen $2s$ and $2p$ σ-bonding orbital.[22]

In analyzing the ^{17}O ENDOR information, we have simply provided the ENDOR frequency and hyperfine coupling (Eq. 2a) from the peak of the ENDOR feature assigned to ^{17}O in Figures 3 and 5. Without additional information, we would take this peak frequency as approximately from an isotropic coupling of ~11–13 MHz magnitude. There should, however, be anisotropy in the μ-oxo ^{17}O hyperfine coupling. A starting point for theoretically estimating hyperfine anisotropy is to calculate the dipolar coupling of the μ-oxo oxygen with electron spin on its Mn(III) and Mn(IV) partners. As explained in the Supporting Information, we applied to μ-oxo ^{17}O the extended point-dipole model originally developed for predicting dipolar hyperfine interactions of protons near the Mn(III)-Mn(IV) with both metal spins,[40, 54, 62] and Figure 8S in the Supporting Information provides a simulation[68] of the μ-oxo ^{17}O ENDOR feature broadened by hyperfine anisotropy. A goal of future advanced EPR studies of ^{17}O in the OEC and models for it should be to resolve this hyperfine anisotropy.

^{17}O ENDOR Assigned to the Terminal Water Ligand on Mn(III) of MnCat

The more weakly coupled $^{17}O_B$ inset to Figure 3B with hyperfine coupling (per Eq. 2a) of about 3.8 MHz became obvious from the MnCat sample that had been exchanged only one minute with ^{17}O-water before freezing. Previous ESEEM[18,69] has provided a hyperfine coupling of about 2 MHz for a ^{17}O-water sharing π–bonding electrons with low-spin ferric heme in an S = ½ system. Because of the +2 projection factor for Mn(III), the hyperfine coupling for π–bonded ^{17}O-water on Mn(III) of the Mn(III)-Mn(IV) pair would be about 4 MHz, comparable to that which is obtained here. The quadrupole tensor of ^{17}O for water ligands of aqua-Mn(II)[70] and aqua-vanadyl complexes,[71] has two large components ($-^{17}P_{xx}$) = $^{17}P_{yy}$ = ~0.33 MHz and a third, $^{17}P_{zz}$ ~ 0. The expected ^{17}O-water quadrupole splittings in the ENDOR expressions of Eq. 2 will be $|3\ ^{17}P_{xx}| \sim |3\ ^{17}P_{yy}| \approx 1$ MHz, comparable with the poorly resolved 1.3 MHz splitting of the shoulders marked in the inset to Figure 3B. We assign the peak feature labeled $^{17}O_B$ to terminal ^{17}O-water on the Mn(III) of the Mn(III)-Mn(IV) pair because there is ENDOR evidence for ^{17}O with hyperfine coupling and possibly quadrupole couplings consistent with water, because there is a terminal water on Mn in the crystal structure of MnCat, and because there are also proton and deuteron ENDOR data consistent with the protons of that very same water. Further, as discussed below, the terminal water, similar in size to the superoxide substrate of MnCat, would be

expected to diffuse into the coordination sphere of the metal center in subsecond times, not hours, and the $^{17}O_B$ feature assigned to terminal water does rapidly appear. We point out that a water σ-bonded along a Jahn-Teller distorted axis of Mn(III) might in principle be expected to have larger hyperfine coupling than water π-bonded to Mn(III) or Mn(IV), but we do not observe a large coupling to a rapidly incorporated ^{17}O.

Exchangeable Proton and Deuteron ENDOR Assigned to the Terminal Water Ligand on Mn(III) of MnCat

The largest proton coupling of 17.2 MHz (singly starred in Figure 4) is comparable to the largest coupling of 17.6 MHz observed from terminal water on Mn(III) from the (2-OH-3,5-Cl$_2$-SALPN)$_2$ Mn(III)-Mn(IV) complex.[54] In the crystal structure of the di-Mn active site in MnCat (Figure 1) there is a carboxylate oxygen of Glu178 within a 2.5 Å hydrogen-bonding distance of the terminal water oxygen with a Mn-O-H-O bond angle of 120°. We have positioned a hydrogen-bonded proton along the water-oxygen-to-carboxylate-oxygen direction at 1.0 Å from the water oxygen. The geometric parameters for that water proton are provided in the Supporting Infomration (See Scheme 1S and pages S11 and S12 in the supporting Information.) The dipolar coupling to this proton is $^1A_{xxdip}$, $^1A_{yydip}$, $^1A_{zzdip}$ = −8.6, −6.6, +15.2 MHz. In addition to the dipolar coupling of $^1A_{zzdip}$ = 15.2 MHz, the total hyperfine coupling of $^1A_{zz}$ = 17.2 MHz of the starred features in Figure 4 would require a small +2.0 MHz isotropic component, comparable to that suggested by Randall *et al.*[54] We assign the proton that gives rise to the observed coupling of 17.2 MHz in Figure 4 to the water that also gives the ^{17}O coupling of 3.8 MHz for $^{17}O_B$. The predicted smaller perpendicular dipolar components, $^1A_{xxdip}$, $^1A_{yydip}$, which are 6–9 MHz in magnitude, would be largely buried here in the proton ENDOR spectra of Figure 4 under non-exchangeable proton ENDOR signals, but the deuteron ENDOR shown in the inset to Figure 4 does have intensity in the 0.9–1.4 MHz region that may correspond to the 6–9 MHz proton region. Water ligated to Mn(III) may have a second proton located further from the Mn(III) than the one with the coupling of 17.2 MHz. Dipolar calculations performed on a second water proton a few tenths of an Å further from the Mn(III) predicted a smaller maximal proton dipolar coupling in the 12–14 MHz range, consistent with the outlying doubly starred proton hyperfine signals having a splitting of 12.2 MHz in Figure 4.

Exchange of Water into the Manganese Active Sites

Q-band ENDOR and X-band EPR showed that the solvent-derived ^{17}O ligands appeared in the di-μ-oxo core of Mn(III)-Mn(IV) bipyridyl[22] within tens of minutes and in the di-μ-oxo core of MnCat within several hours. Q-band ^{17}O ENDOR and Resonance-Raman-detectable ^{18}O at a μ-oxo site[23] within PSII occurred on a similar time scale. If the μ-oxo ^{17}O observed by ENDOR of PSII is the same μ-oxo that Resonance Raman has resolved after slow exchange,[23] then this oxygen would not be catalytically relevant in the sense that it rapidly appears in the O$_2$ product, although it is relevant to the structure of the catalytic center. (It is likely that the bridge opening to allow oxygen exchange requires a proton from a nearby base,[24] such as a nearby arginine in the OEC.)

MnCat functions with a time for superoxide turnover of 5 μs, close to the diffusion limit.[30] Superoxide, and very likely the similar-sized water, can diffuse into the active site very easily, so that diffusion of water into the interior of the MnCat hexamer,[27] as opposed to exchange into the μ-oxo Mn(III)-Mn(IV) core, is unlikely to be an impediment to oxygen isotope exchange for MnCat. The evidence for terminal water ligation from H$_2$$^{17}O$ samples frozen within a minute of the initiation of water exchange, is consistent with such a rapid exchange, which indeed may even occur in a much shorter time than a minute.

The large ENDOR-resolved proton coupling in MnCat ($^1A_{zz} > 15$ MHz) indicating ligation of a terminal water to Mn(III) of the di-μ-oxo Mn(III)-Mn(IV) pair in MnCat has not yet been observed in PSII. We would interpret the hyperfine couplings of so far unresolved exchangeable proton/deuterons in the OEC derived from ENDOR and ESEEM,[72, 73] as being too small to be those of water protons on a Mn(III) of a Mn(III)-Mn(IV) antiferromagnetically coupled pair. We cannot at this point exclude hydrogen bonding to a bridging μ-oxo between Mn and Ca as a candidate for ESEEM-observable hydrogen bonds in PSII because to date there is not a Mn-Ca model to test this hypothesis.

Conclusion

Although there was previous ENDOR evidence for exchange of ^{17}O from ^{17}O-water into the μ-oxo ligands of the Mn(III)-Mn(IV) bipyridine model complex,[21, 22, 24] the spectroscopic signatures had not been explored for ^{17}O exchanged from ^{17}O-water into a protein active site having the potential to exchange both μ-oxo and terminal water oxygens. MnCat, di-μ-oxo Mn(III)-Mn(IV) bipyridine, and the S_2 signal of the OEC have now all provided a similar ^{17}O ENDOR signal that arose after slow exchange with ^{17}O-water. This signal is assigned to a μ-oxo oxygen that joins a Mn(III)-Mn(IV) antiferromagnetically coupled pair. This μ-oxo oxygen, an important structural aspect of multi-Mn centers, exchanged on the scale of tens of minutes into the Mn(III)-Mn(IV) bipyridine complex and on the time scale of hours into the μ-oxo Mn(III)-Mn(IV) centers of MnCat and the OEC. Thus, the rapid water binding sites for the OEC are most likely to be terminal, or even more distant, water binding sites. As judged by the small magnitude of exchangeable ^1H and ^2H hyperfine couplings for the OEC[72,73] when compared to the > 15 MHz exchangeable proton coupling from the assigned terminal water ligand of Mn(III) in Mn(III)-Mn(IV) MnCat, these sites in the OEC are not of a terminal water to the Mn(III) of a Mn(III)-Mn(IV) pair. Hydrogen bonding to a μ-oxo ligand between Mn and Ca cannot be excluded.

For MnCat, ENDOR evidence was obtained for terminal water exchange with $H_2^{17}O$ on a minute (or less) time scale. ^{17}O hyperfine and possible ^{17}O quadrupole ENDOR signals, which differed significantly from ^{17}O-μ-oxo ENDOR signals, indicated terminal water. In addition there were large exchangeable proton couplings consistent with the dipole interaction of a water ligand proton with a near Mn(III) and a more distant Mn(IV); exchangeable deuteron signals, although less well resolved, were also consistent with the deuterium on the same terminal water.

In Scheme 1 we succinctly present the outcomes reported in this article. Scheme 1 summarizes the time span for the appearance of ^{17}O-ENDOR peak positions from MnCat and the OEC and for our assignment of the physical location of these ^{17}O within the manganese centers of MnCat and the OEC. The assignment of exchangeable proton/deuteron ENDOR to the exchangeable water on the Mn(III) of MnCat is also noted.

Supplementary Material

Refer to Web version on PubMed Central for supplementary material.

Acknowledgments

References

1. McConnell I, Li G, Brudvig GW. Chemistry and Biology. 2010; 17:434–447. [PubMed: 20534342]

2. Moore GF, Brudvig GW. Annu Rev Condensed Matter Phys. 2011; 2:303–327.

3. Lewis NS, Nocera DG. Proc Natl Acad Sci U S A. 2006; 103:15729–15735. [PubMed: 17043226]

4. Lewis NS. MRS Bull. 2007; 32:808–820.

5. Lewis NS. Science. 2007; 315:798–801. [PubMed: 17289986]

6. McEvoy JP, Brudvig GW. Chem Rev. 2006; 106:4455–4483. [PubMed: 17091926]

7. Ferreira KN, Iverson TM, Maghlaoui K, Barber J, Iwata S. Science. 2004; 303:1831–1838. [PubMed: 14764885]

8. Guskov A, Kern J, Gabdulkhakov A, Broser M, Zouni A, Saenger W. Nat Struct Mol Biol. 2009; 16:334–342. [PubMed: 19219048]

9. Umena Y, Kawakami K, Shen J-R, Kamiya N. Nature. 2011; 472:55–60. [PubMed: 21499260]

10. Messinger J, Badger M, Wydrzynski T. Proc Natl Acad Sci U S A. 1995; 92:3209–3213. [PubMed: 11607525]

11. Hillier W, Messinger J, Wydrzynski T. Biochemistry. 1998; 37:16908–16914. [PubMed: 9836583]

12. Hillier W, Wydrzynski T. Biochemistry. 2000; 39:4399–4405. [PubMed: 10757989]

13. Hillier W, Wydrzynski T. Physical Chemistry Chemical Physics. 2004; 6:4882–4889.

14. Hillier W, Wydrzynski T. Coordination Chemistry Reviews. 2008; 252:306–317.

15. Dismukes GC, Siderer Y. FEBS lett. 1980; 121:78–80.

16. Hansson Ö, Andréasson L-E, Vänngård T. FEBS lett. 1986; 195:151–154.

17. Evans MC, Nugent JH, Ball RJ, Muhiuddin I, Pace RJ. Biochemistry. 2004; 43:989–994. [PubMed: 14744143]

18. Goldfarb D, Bernardo M, Thomann H, Kroneck PMH, Ullrich V. J Am Chem Soc. 1996; 118:2686–2693.

19. Su JH, Lubitz W, Messinger J. Am Chem Soc. 2008; 130:786–787.

20. Su JH, Lubitz W, Messinger J. J Am Chem Soc. 2011; 133:12317.

21. Tagore R, Chen HY, Crabtree RH, Brudvig GW. J Am Chem Soc. 2006; 128:9457–9465. [PubMed: 16848483]

22. Usov OM, Grigoryants VM, Tagore R, Brudvig GW, Scholes CP. Journal of the American Chemical Society. 2007; 129:11886–11887. [PubMed: 17850079]

23. Chu HA, Sackett H, Babcock GT. Biochemistry. 2000; 39:14371–14376. [PubMed: 11087389]

24. Tagore R, Crabtree RH, Brudvig GW. Inorganic Chemistry. 2007; 46:2193–2203. [PubMed: 17295472]

25. Kono Y, Fridovich I. J Biol Chem. 1983; 258:6015–6019. [PubMed: 6853475]

26. Barynin VV, Vagin AA, Melik-Adamyan VR, Grebenko AI, Khangulov SV, Popov AN, Andrianova ME, Vainshtein BK. Sov Phys-Dokl (Engl Transl). 1986; 31:457–459.

27. Barynin VV, Whittaker MM, Antonyuk SV, Lamzin VS, Harrison PM, Artymiuk PJ, Whittaker JW. Structure. 2001; 9:725–738. [PubMed: 11587647]

28. Waldo GS, Yu S, Penner-Hahn JE. J Am Chem Soc. 1992; 114:5869–5870.

29. Waldo GS, Penner-Hahn JE. Biochemistry. 1995; 34:1507–1512. [PubMed: 7849009]

30. Wu AJ, Penner-Hahn JE, Pecoraro VL. Chem Rev. 2004; 104:903–938. [PubMed: 14871145]

31. Waldo GS, Fronko RM, Penner-Hahn JE. Biochemistry. 1991; 30:10486–10490. [PubMed: 1657146]

32. Khangulov SV, Barynin VV, Antonyuk-Barynina SV. Biochim Biophys Acta. 1990; 1020:25–33.

33. Khangulov SV, Barynin VV, Voevodskaya NV, Grebenko AI. Biochim Biophys Acta. 1990; 1020:305–310.

34. Whittaker MM, Barynin VV, Antonyuk SV, Whittaker JW. Biochemistry. 1999; 38:9126–9136. [PubMed: 10413487]

35. Meier AE, Whittaker MM, Whittaker JW. Biochemistry. 1996; 35:348–360. [PubMed: 8555195]

36. Schäfer K-O, Bittl R, Lendzian F, Barynin V, Weyhermller T, Wieghardt K, Lubitz W. J Phys Chem B. 2003; 107:1242–1250.

37. Stemmler TL, Sturgeon BE, Randall DW, Britt RD, Penner-Hahn JE. J Am Chem Soc. 1997; 119:9215–9225.

38. Larson E, Lah MS, Li X, Bonadies JA, Pecoraro VL. Inorg Chem. 1992; 31:373–378.

39. Stich TA, Whittaker JW, Britt RD. J Phys Chem B. 2010; 114:14178–14188. [PubMed: 20055466]

40. Khangulov S, Sivaraja M, Barynin VV, Dismukes GC. Biochemistry. 1993; 32:4912–4924. [PubMed: 8387822]

41. Fronko RM, Penner-Hahn JE, Bender CJ. J Am Chem Soc. 1988; 110:7554–7555.

42. Berthold DA, Babcock GT, Yocum CF. FEBS lett. 1981; 134:231–234.

43. Sienkiewicz A, Smith BG, Veselov A, Scholes CP. Rev of Sci Instrum. 1996; 67:2134–2138.

44. Lee B, Usov OM, Grigoryants VM, Myers WK, Shapleigh JP, Scholes CP. Biochemistry. 2009; 48:8985–8993. [PubMed: 19685879]

45. Zhao Y, Lukoyanov DA, Toropov YV, Wu K, Shapleigh JP, Scholes CP. Biochemistry. 2002; 41:7464–7474. [PubMed: 12044180]

46. Burdi D, Willems J-P, Riggs-Gelasco P, Antholine WE, Stubbe J, Hoffman BM. J Am Chem Soc. 1998; 120:12910–12919.

47. Willems J-P, Lee H-I, Burdi D, Doan PE, Stubbe J, Hoffman BM. J Am Chem Soc. 1997; 119:9816–9824.

48. Usov OM, Choi PS, Shapleigh JP, Scholes CP. J Am Chem Soc. 2006; 128:5021–5032. [PubMed: 16608336]

49. Myers WK, Scholes CP, Tierney DL. J Am Chem Soc. 2009; 131:10421–10429. [PubMed: 19591466]

50. Werst MM, Kennedy MC, Beinert H, Hoffman BM. Biochemistry. 1990; 29:10526–10532. [PubMed: 2176871]

51. Veselov A, Sun H, Sienkiewicz A, Taylor H, Burger RM, Scholes CP. J Am Chem Soc. 1995; 117:7508–7512.

52. Veselov AV, Osborne JP, Gennis RB, Scholes CP. J Am Chem Soc. 2000; 122:8712–8716.

53. Hoffman, BM.; DeRose, VJ.; Doan, PE.; Gurbiel, RJ.; Houseman, ALP.; Telser, J. Biological Magnetic Resonance, Vol. 13: EMR of Paramagnetic Molecules. Berliner, LJ.; Reuben, J., editors. Vol. 13. Plenum; New York: 1993.

54. Randall DW, Gelasco A, Caudle MT, Pecoraro VL, Britt RD. J Am Chem Soc. 1997; 119:4481–4491.

55. Yeagle GJ, Gilchrist ML Jr, Walker LM, Debus RJ, Britt RD. Philos Trans R Soc Lond B Biol Sci. 2008; 363:1157–1166. discussion 1166. [PubMed: 17954435]

56. Yeagle GJ, Gilchrist ML, McCarrick RM, Britt RD. Inorg Chem. 2008; 47:1803–1814. [PubMed: 18330971]

57. Sproviero EM, Gascon JA, McEvoy JP, Brudvig GW, Batista VS. J Am Chem Soc. 2008; 130:3428–3442. [PubMed: 18290643]

58. Kulik LV, Epel B, Lubitz W, Messinger J. J Am Chem Soc. 2007; 129:13421–13435. [PubMed: 17927172]

59. Peloquin JM, Campbell KA, Randall DW, Evanchik MA, Pecoraro VL, Armstrong WH, Britt RD. J Am Chem Soc. 2000; 122:10926–10942.

60. Anderson, PW. Exchange in Insulators: Superexchange, Direct Exchange, and Double Exchange. In: Rado, GT.; Suhl, H., editors. Magnetism. Vol. I. Academic Press; New York: 1963. p. 28-83.

61. Noodleman L, Peng CY, Case DA, Mouesca JM. Coord Chem Rev. 1995; 144:199–244.

62. Sinnecker S, Neese F, Noodleman L, Lubitz W. J Am Chem Soc. 2004; 126:2613–2622. [PubMed: 14982471]

63. Sinnecker S, Neese F, Lubitz W. J Biol Inorg Chem. 2005; 10:231–238. [PubMed: 15830216]

64. Schinzel S, Kaupp M. Can J Chem. 2009; 87:1521–1539.

65. Pantazis DA, Orio M, Petrenko T, Zein S, Lubitz W, Messinger J, Neese F. Phys Chem Chem Phys. 2009; 11:6788–6798. [PubMed: 19639153]

66. Burdi D, Sturgeon BE, Tong WH, Stubbe J, Hoffman BM. J Am Chem Soc. 1996; 118:281–282.

67. Sturgeon BE, Burdi D, Chen S, Huynh B-H, Edmondson DE, Stubbe J, Hoffman BM. J Am Chem Soc. 1996; 118:7551–7557.

68. Stoll S, Schweiger A. J Magn Reson. 2006; 178:42–55. [PubMed: 16188474]

69. Thomann H, Bernardo M, Goldfarb D, Kroneck PMH, Ullrich V. J Am Chem Soc. 1995; 117:8243–8251.

70. Tan X, Bernardo M, Thomann H, Scholes CP. J Chem Phys. 1995; 102:2675–2690.

71. Baute D, Goldfarb D. J Phys Chem A. 2005; 109:7865–7871. [PubMed: 16834167]

72. Britt RD, Campbell KA, Peloquin JM, Gilchrist ML, Aznar CP, Dicus MM, Robblee J, Messinger J. Biochim Biophys Acta. 2004; 1655:158–171. [PubMed: 15100028]

73. Su JH, Messinger J. Appl Magn Reson. 2010; 37:123–136. [PubMed: 19960065]
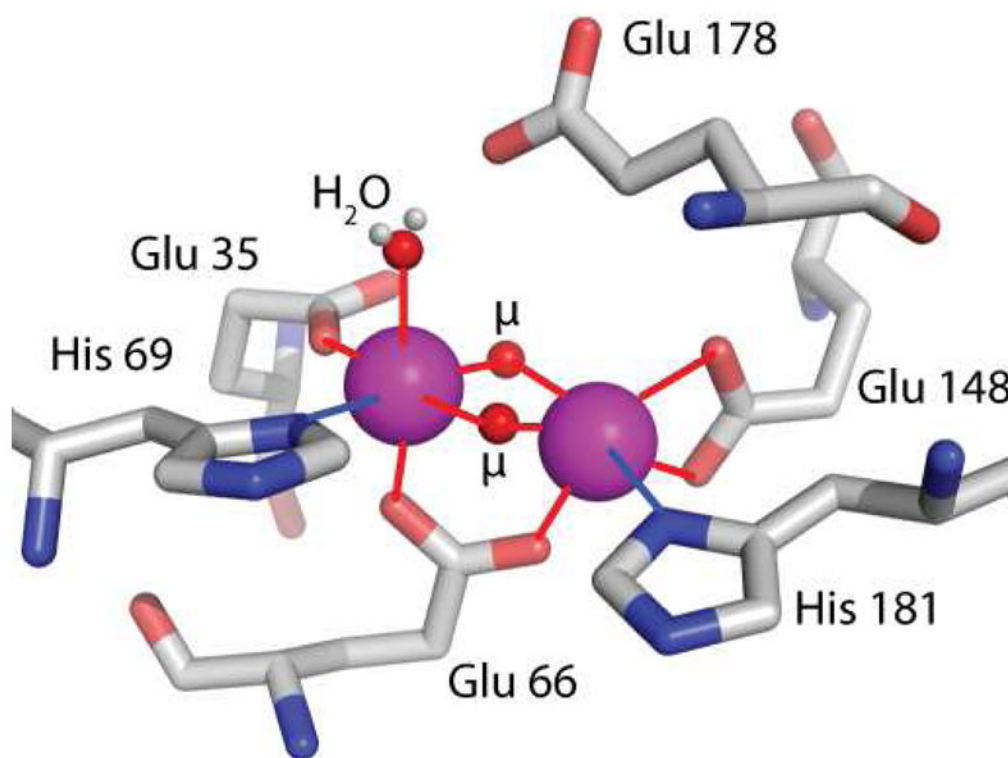
Figure 1.
Shown is the local liganding environment of the di-manganese center of MnCat from *L. plantarum*. The structure is taken from the X-ray crystallographic structure of the Mn(III)-Mn(III) derivative, PDB structure 1JKU.[27] Glu178 does not directly ligate the manganese but is within hydrogen bonding distance (2.5 Å) of the liganding water oxygen. The μ labels indicate solvent derived ligands. It is expected that there would be two μ-oxos in the (III,IV) form, and potentially a μ-oxo and μ-OH in the (III,III) state.[27]
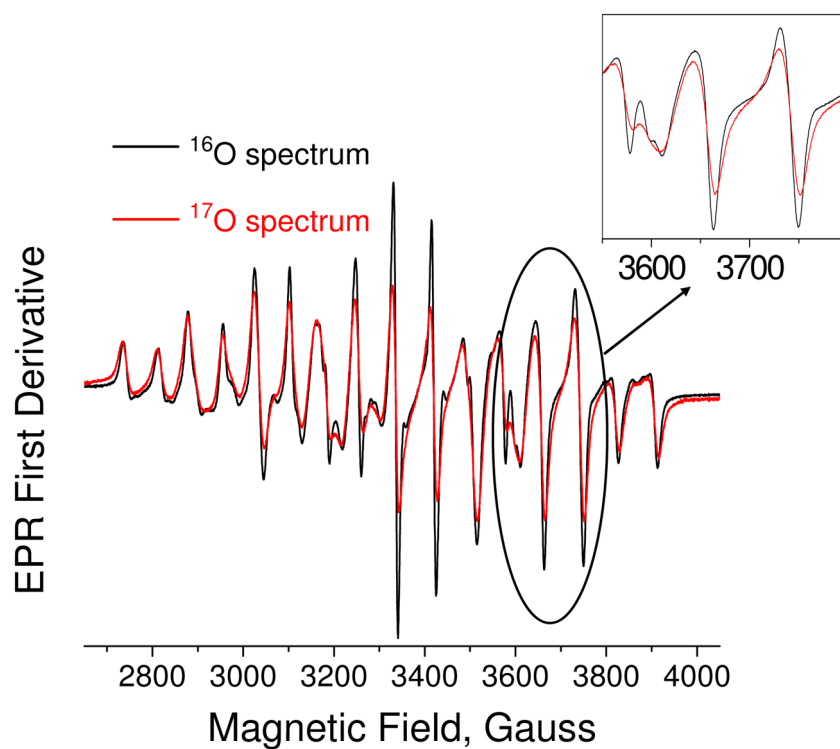
Figure 2.
CW first derivative X-band EPR spectra are presented for MnCat exchanged in $H_2{}^{16}O$ (black) and 90% $H_2{}^{17}O$ (red). The inset shows an enlarged view of several hyperfine lines to demonstrate the broadening. The spectra from the MnCat in $H_2{}^{16}O$ and 90% $H_2{}^{17}O$ have been normalized to the integrated spin count. Samples were incubated for two hours after addition of labeled or non-labeled water before freezing.
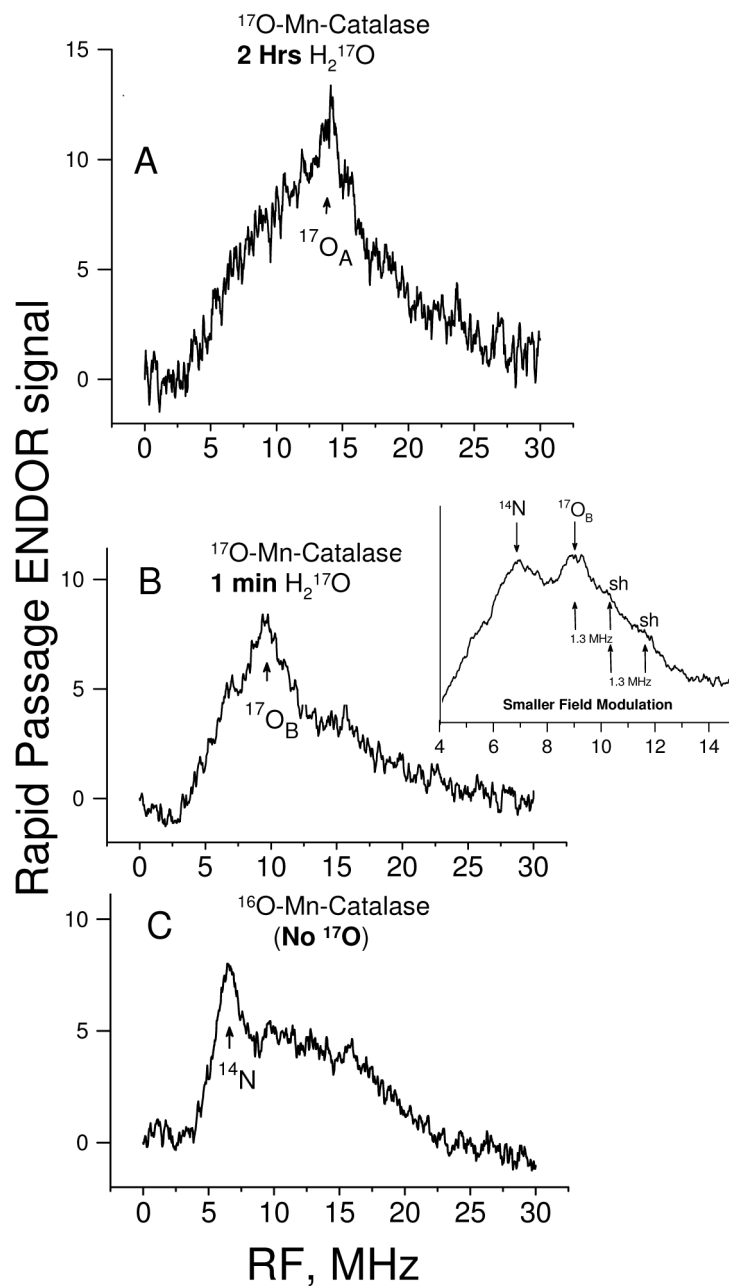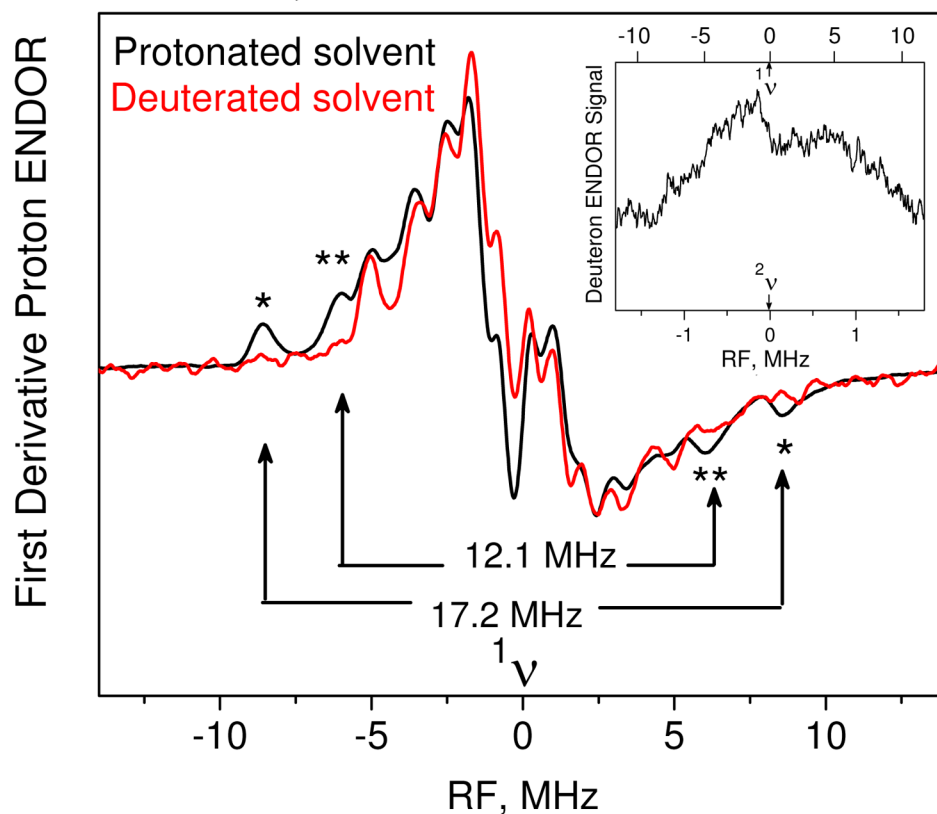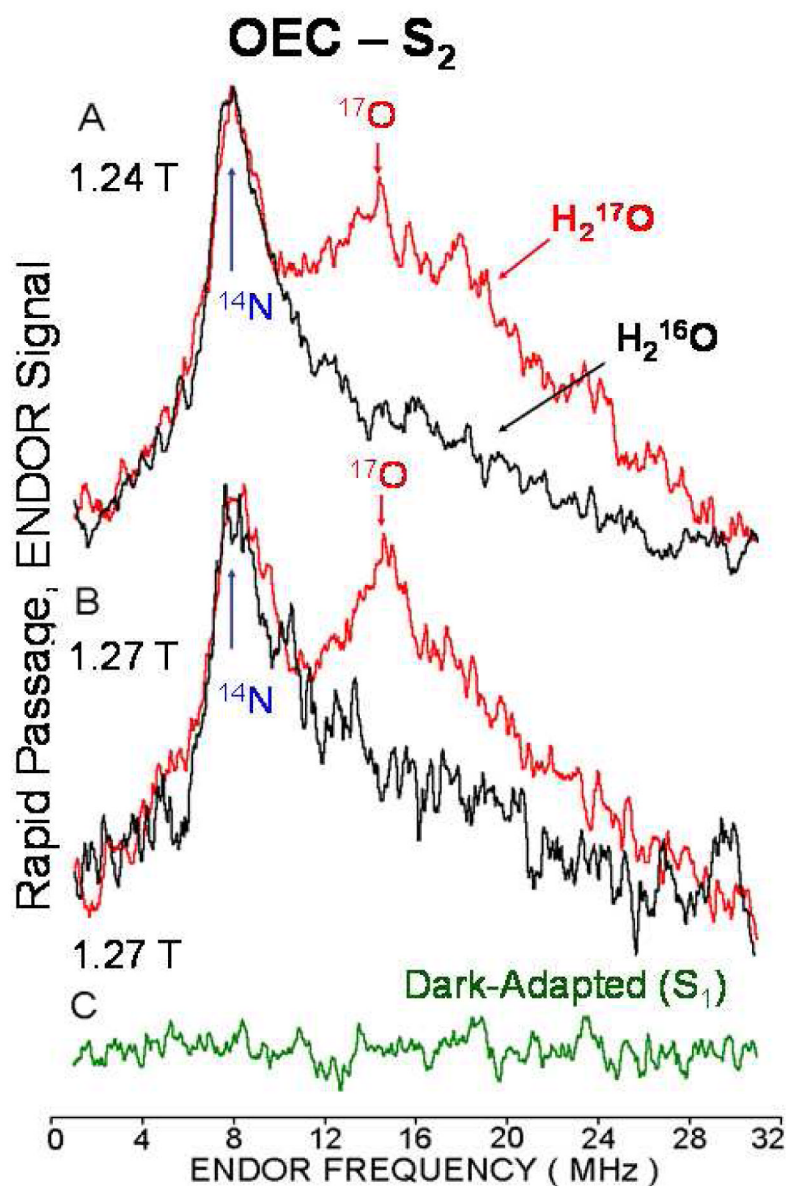
Figure 3.
This figure provides a comparison of the ENDOR signals in the 1–30 MHz range from MnCat prepared as follows: **A**) in 66 % [17]O-water with a two hour incubation before freezing; **B**) in 66% [17]O water with a 1 min incubation before freezing; C) ^{16}O-water. These spectra were obtained at a magnetic field of 1.243 T. Conditions: microwave power = 0.22 μW, modulation amplitude = 5 G p.t.p., time constant = 20 ms, RF power ≈ 10 W, sweep rate = 6 MHz/s. Spectrum **A** was the result of 3300 5 s sweeps, and **B** and **C** were the result of 1000 5 s sweeps. Spectra **A**, **B**, and **C** were normalized to the number of sweeps and to their respective underlying EPR intensities, and the vertical intensity unit scale is the same for A, B, and C. Inset: The inset was obtained from MnCat exchanged in [17]O-water for 1 minute, but to obtain better resolution of weakly coupled features, a field modulation of 2.5

Gauss p.t.p., a slower sweep of 3 MHz/s over a 1–16 MHz range, and a higher RF power by a factor of 2. The inset spectrum was the result of 1100 5 s sweeps.

## Mn Catalase, Protonated versus Deuterated Solvent

Figure 4.
This figure presents the first derivative [1]H-ENDOR spectra, centered at the free proton NMR frequency, $^1\nu$, to compare exchangeable features from MnCat prepared in protonated solution with MnCat prepared in deuterated solution. Conditions: 1.243 T ($^1\nu$ = 52.92 MHz), microwave power = 0.22 μW, field modulation = 5 G p.t.p., time constant = 20 ms, sweep rate = 3 MHz/s, 750 scans for the protonated sample and 250 for the deuterated sample. *Inset:* [2]H-ENDOR of D_2O-exchanged MnCat following subtraction of the underlying spectrum from a protonated MnCat sample. Deuteron ENDOR conditions: ($^2\nu$ = 8.12 MHz), sweep rate = 1 MHz/s, field modulation = 0.5 G p.t.p., scans = 1000. The inset spectrum is centered at the free deuteron NMR frequency, and the scale above it is the proton frequency scale (obtained with a multiplier of 6.52) corresponding to the deuteron scale. Exchange of D_2O was accomplished in about a minute and the sample frozen; the sample was then unfrozen, deuterated glycerol added, and refrozen in about 5 minutes.

Figure 5.
ENDOR spectra of white light-illuminated PSII in $H_2^{17}O$ (red) and $H_2^{16}O$ (black) and a dark-adapted sample in $H_2^{17}O$ (green) at field positions: (A) 1.24 T and (B) & (C) 1.27 T. A light-induced feature ($^{17}\nu^+$ENDOR) from the ^{17}O sample occurs at 12.8 ± 1.0 MHz. Acquisition conditions: field modulation 2.5 G, time constant 82 msec, mw power = 0.28 μW, RF sweep rate 3 MHz/sec, number of scans (A) 1200, (B) 600, and (C) 200. Spectral amplitudes were normalized to the peak labeled 14N. Quoted ENDOR and hyperfine frequencies in text are the average of upward and downward frequency sweeps shown in the Supporting Information, Figure 7S.
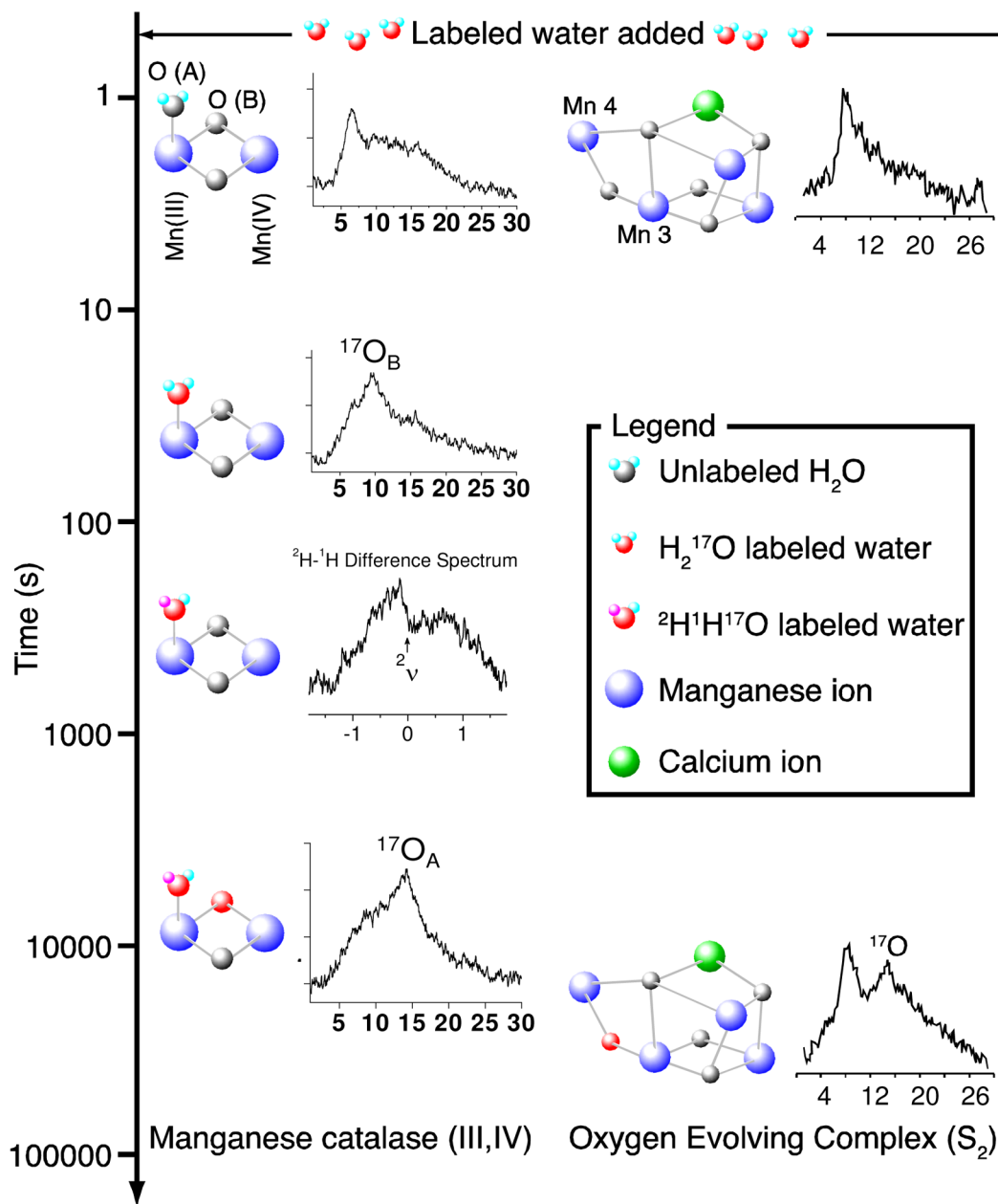
Scheme 1.
shows the following information: a) The time course for $H_2{}^{17}O$ binding and ^{17}O-migration within the limits of the present experiments. b) The location of the ^{17}O peaks as the time course of the experiment progresses., including the labels $^{17}O_A$ for μ-oxo and $^{17}O_B$ from a ^{17}O-water ligand. c) The location of the exchangeable H on terminal water ligand of Mn(III) in MnCat. is shown. d) The labels of Mn(4) and Mn(3) are indicated per Sproviero et al. [55]